

Distinct pathways leading to TDP-43-induced cellular dysfunctions

Makiko Yamashita¹, Takashi Nonaka^{1,*}, Shinobu Hirai², Akiko Miwa², Haruo Okado², Tetsuaki Arai⁴, Masato Hosokawa³, Haruhiko Akiyama³ and Masato Hasegawa^{1,*}

¹Department of Neuropathology and Cell Biology, ²Department of Brain Development and Neural Regeneration and ³Dementia Research Project, Tokyo Metropolitan Institute of Medical Science, Tokyo 156-8506, Japan and ⁴Department of Neuropsychiatry, Division of Clinical Medicine, Faculty of Medicine, University of Tsukuba, Tsukuba, Ibaraki 305-8575, Japan

Received February 10, 2014; Revised February 10, 2014; Accepted March 31, 2014

TAR DNA-binding protein of 43 kDa (TDP-43) is the major component protein of inclusions found in brains of patients with amyotrophic lateral sclerosis (ALS) and frontotemporal lobar degeneration (FTLD-TDP). However, the molecular mechanisms by which TDP-43 causes neuronal dysfunction and death remain unknown. Here, we report distinct cytotoxic effects of full-length TDP-43 (FL-TDP) and its C-terminal fragment (CTF) in SH-SY5Y cells. When FL-TDP was overexpressed in the cells using a lentiviral system, exogenous TDP-43, like endogenous TDP-43, was expressed mainly in nuclei of cells without any intracellular inclusions. However, these cells showed striking cell death, caspase activation and growth arrest at G2/M phase, indicating that even simple overexpression of TDP-43 induces cellular dysfunctions leading to apoptosis. On the other hand, cells expressing TDP-43 CTF showed cytoplasmic aggregates but without significant cell death, compared with cells expressing FL-TDP. Confocal microscopic analyses revealed that RNA polymerase II (RNA pol II) and several transcription factors, such as specificity protein 1 and cAMP-response-element-binding protein, were co-localized with the aggregates of TDP-43 CTF, suggesting that sequestration of these factors into TDP-43 aggregates caused transcriptional dysregulation. Indeed, accumulation of RNA pol II at TDP-43 inclusions was detected in brains of patients with FTLD-TDP. Furthermore, apoptosis was not observed in affected neurons of FTLD-TDP brains containing phosphorylated and aggregated TDP-43 pathology. Our results suggest that different pathways of TDP-43-induced cellular dysfunction may contribute to the degeneration cascades involved in the onset of ALS and FTLD-TDP.

INTRODUCTION

TAR DNA-binding protein of 43 kDa (TDP-43) has been identified as a major component protein of the ubiquitinated inclusions characteristic of amyotrophic lateral sclerosis (ALS) and frontotemporal lobar degeneration with ubiquitin-positive inclusions (FTLD-U or FTLD-TDP) (1,2). TDP-43 is a ubiquitously expressed nuclear protein and is implicated in exon splicing, gene transcription, regulation of mRNA stability and biosynthesis and formation of nuclear bodies (3–7). It is a 414-amino acid protein with two highly conserved RNA recognition motifs (RRM1 and RRM2) and a glycine-rich region

mediating protein–protein interactions at the C-terminus (8–11). In TDP-43 proteinopathy, pathological TDP-43 is abnormally phosphorylated, ubiquitinated and N-terminally cleaved to generate C-terminal fragments (CTFs) (1,12,13).

As autosomal-dominant missense mutations in the *TARDBP* gene were identified in patients with ALS or FTLD-TDP, toxic gain of function of TDP-43 may be related to neuronal degeneration. However, in most cases of TDP-43 proteinopathy, no *TARDBP* mutations are identified, suggesting that wild-type TDP-43 itself is central to the disease cascade. A 2-fold increase in total *TARDBP* mRNA was reported in a 3'-untranslated region variant carrier (14), which suggests that just an increased level of

*To whom correspondence should be addressed at: Department of Neuropathology and Cell Biology, Tokyo Metropolitan Institute of Medical Science, 2-1-6, Kamikitazawa, Setagaya-ku, Tokyo 156-8506, Japan. Tel: +81 36834 2349; Fax: +81 36834 2349; Email: nonaka-tk@igakuken.or.jp (T.N.), hasegawa-ms@igakuken.or.jp (M.H.)

TDP-43 protein (22%) can cause FTL-D-TDP. Similarly, overexpression of wild-type TDP-43 causes motor neuron degeneration in yeast, mice and rats (15–17). Moreover, it has recently been reported that the C-terminal portion of TDP-43 shows sequence similarity to prion protein (18) and that truncated CTFs of TDP-43 readily form intracellular aggregates in cultured cells (19–21), suggesting that not only FL-TDP but also its CTFs contribute to the pathogenesis of TDP-43 proteinopathy. However, the molecular mechanisms through which FL-TDP or aggregated CTFs cause neuronal dysfunctions leading to cell death remain unknown. To identify the mechanisms involved, we examined whether overexpression of FL-TDP or its CTF induced cell death in human neuroblastoma line SH-SY5Y cells. We report here that two different pathways lead to cellular dysfunctions induced by FL-TDP and by its CTF. We observed striking apoptotic cell death and cell cycle arrest at the G2/M phase in cells overexpressing FL-TDP. In cells overexpressing TDP-43 CTF, RNA polymerase II (RNA pol II) and several transcription factors such as specificity protein 1 (Sp1) and cAMP-response-element-binding protein (CREB) were co-localized with cytoplasmic aggregates of TDP-43 CTF and their transcriptional activities were decreased, although apoptotic cell death was not significant. These results suggest that recruitment of these factors may cause transcriptional dysregulation, thereby leading to cellular dysfunctions. Dysregulation of FL-TDP expression and/or cytoplasmic accumulation of TDP-43 CTF may contribute to the pathogenesis of ALS and FTL-D-TDP.

RESULTS

Overexpression of FL-TDP or its CTF causes cellular dysfunctions in SH-SY5Y cells

Gitcho *et al.* (14) reported a 2-fold increase in total expression of *TARDBP* in a 3'-untranslated region variant carrier of FTL-D-TDP, and mice or yeasts overexpressing human TDP-43 develop various abnormalities, including cytotoxicity, neuronal loss and motor deficits (15,17). These findings suggest that overexpression of TDP-43 can cause neuronal degeneration *in vivo*. However, no striking cell death was detected in cultured SH-SY5Y cells transiently expressing a plasmid encoding FL-TDP (20,22). Therefore, to examine whether more substantial and stable expression of TDP-43 is required for induction of its cytotoxic effect in cultured cells, we used a lentiviral system for expression of TDP-43. We prepared SH-SY5Y cells stably expressing FL-TDP (FL-TDP), a deletion mutant of the nuclear localization signal [Δ NLS-TDP; 78–84 residues (23)] and CTF of TDP-43 [C-TDP; 162–414 residues (20)], by using a lentiviral expression system (Fig. 1A). At 3 days after infection, transfected cells were subjected to immunohistochemical and biochemical analyses. Confocal microscopic analyses (Fig. 1B) showed that FL-TDP was expressed mainly in nuclei, but was not phosphorylated or aggregated. Δ NLS-TDP was expressed mainly in cytoplasm, without phosphorylation or aggregation. In cells expressing C-TDP, phosphorylated and aggregated C-TDP was detected with phospho-TDP-43 specific antibody, anti-pS409/410 (Fig. 1B). Immunoblot analyses of transfected cell lysates also revealed that FL-TDP and Δ NLS-TDP were recovered mainly in Triton X-100 (TX)-sup fraction without phosphorylation, while C-TDP was phosphorylated and aggregated in TX-ppt fraction, as shown in Figure 1C.

We examined the cytotoxic effects of these TDP-43 constructs in SH-SY5Y cells. At 4 days after lentiviral infection, the viability of cells transfected with FL-TDP was strongly suppressed and striking cell death was observed (Fig. 2A–C), suggesting that expression of FL-TDP is highly cytotoxic for SH-SY5Y cells. As shown in Figure 2D, poly(ADP-ribose) polymerase (PARP), a well-known substrate for activated caspase-3, was cleaved in cells expressing FL-TDP. This result clearly indicates that expression of FL-TDP induces apoptotic cell death. On the other hand, expression of Δ NLS-TDP or C-TDP did not influence the viability at 4–7 days (Fig. 2B). We also found that expression of the N-terminal fragment of TDP-43 (N-TDP: 1–161 residues) has no cytotoxic effect (Supplementary Material, Fig. S1). In cells expressing C-TDP, however, the number of living cells was significantly less than that in mock cells or cells expressing Δ NLS-TDP at 7 days (Fig. 2C). These results suggest that expression of not only FL-TDP but also CTF of TDP-43 causes cellular dysfunctions in SH-SY5Y cells, and may indicate that expression of FL-TDP without aggregate formation and expression of CTF with inclusions induce cellular damage through distinct mechanisms.

Different modes by which FL-TDP and its CTF induce cellular dysfunctions

To examine this possibility, we performed BrdU incorporation assay in cells expressing green fluorescent protein (GFP)-tagged FL-TDP (GFP-FL-TDP) or CTF (GFP-C-TDP) (Fig. 3A). Since stable expression of TDP-43 using the lentiviral system often resulted in severe damage to SH-SY5Y cells, we mainly used cells transiently expressing TDP-43 plasmids in subsequent work. SH-SY5Y cells were transfected with a plasmid encoding GFP-FL-TDP or GFP-C-TDP for 3 days, then treated with BrdU. After 10 h incubation, the cells were fixed and stained with anti-BrdU antibody and observed with a confocal microscope. As shown in Figure 3B and C, incorporation of BrdU in cells expressing GFP-FL-TDP was significantly decreased when compared with that in cells expressing the empty vector (pEGFP), indicating that DNA synthesis and cell growth were suppressed by overexpression of GFP-FL-TDP. We also found that cells with diffuse expression of GFP-C-TDP were stained with anti-BrdU antibody, while cells including GFP-C-TDP aggregates were not (Fig. 3B, right). Quantitative analysis showed that BrdU incorporation was almost wholly suppressed in cells with GFP-C-TDP inclusions (Fig. 3C). These results indicate that suppression of cell growth owing to formation of GFP-C-TDP inclusions is more marked than that owing to expression of GFP-FL-TDP or GFP-C-TDP without inclusions.

Next, we analyzed the cell cycle by measuring the DNA content of propidium iodide (PI)-stained cells. SH-SY5Y cells were transfected with GFP-FL-TDP or GFP-C-TDP. Three days after transfection, cells were stained with PI and analyzed using a flow cytometer. As shown in Figure 4A and B, cells transfected with GFP-FL-TDP were extensively accumulated in the G2/M and subG1 phases when compared with those transfected with empty vector (pEGFP) or GFP-C-TDP. It is well known that apoptotic cells are accumulated in the subG1 phase, and an increase of cells in the G2/M phase reflects growth arrest, leading to apoptosis. This result shows that overexpression of GFP-FL-TDP induces apoptosis, which is consistent with the

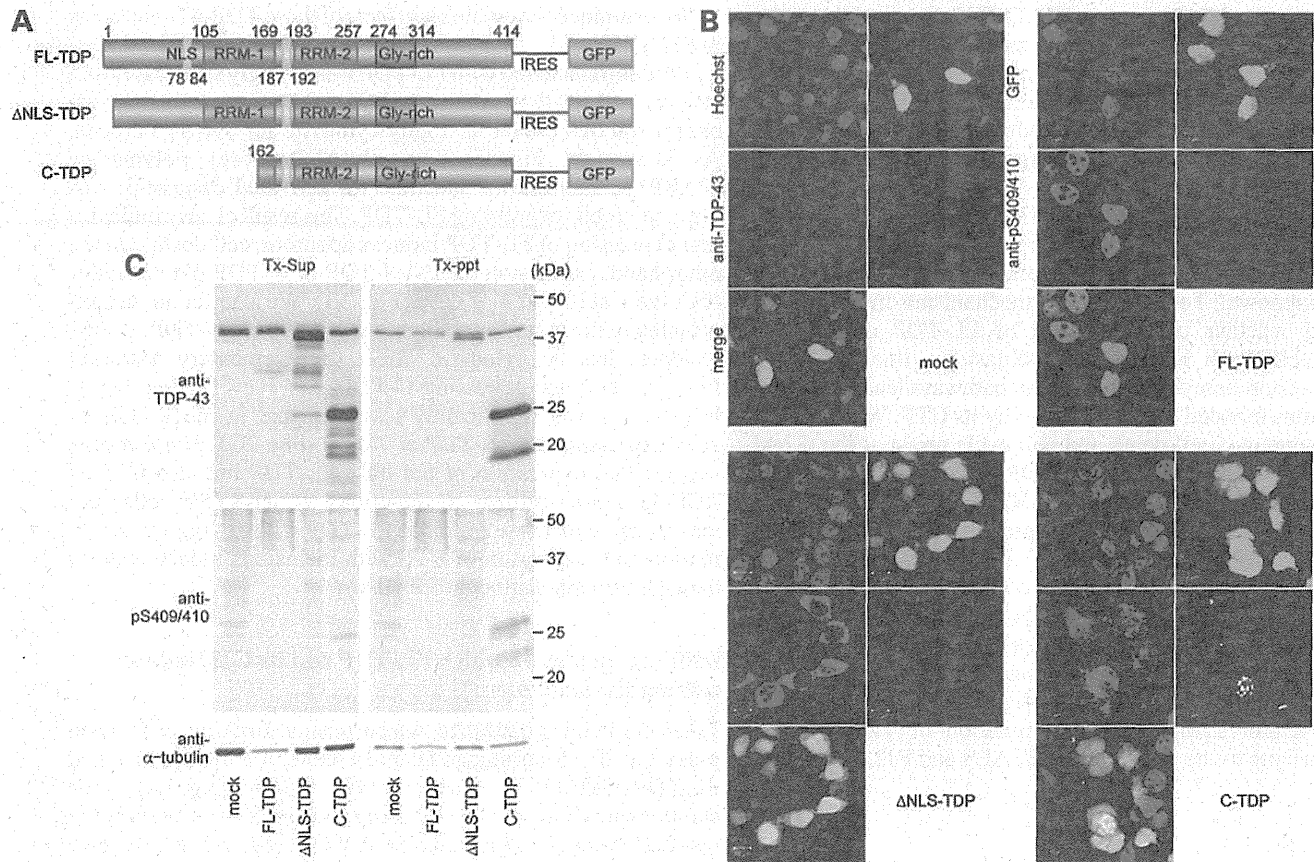


Figure 1. Overexpression of TDP-43 constructs in SH-SY5Y cells. (A) Schematic representation of FL-TDP, TDP-43 with deletion of the nuclear localization signal [78–84 residues (23)] (ΔNLS-TDP) and CTF (C-TDP) constructs in lentiviral expression system. RNA recognition motifs (RRM-1 and RRM-2; blue) and glycine-rich domain (Gly-rich; red) are shown. (B) SH-SY5Y cells were infected with each TDP-43 virus at 2×10^7 copies/well. At 4 days after infection, the cells were fixed and stained with anti-TDP-43 and anti-phospho-TDP-43 (anti-pS409/410) antibodies. Scale bars, 10 μm. (C) Transfected cells were also prepared for western blotting (20, 22). Cell lysates were extracted with 1% Triton X-100 (Tx), and the supernatants (Tx-sup) and insoluble pellets (Tx-ppt) after centrifugation at 100 000g for 20 min were analyzed by immunoblotting. The blots were probed with anti-TDP-43, anti-pS409/410 or anti-tubulin antibody.

result obtained in the case of lentiviral expression of FL-TDP (Fig. 2D). On the other hand, the cell cycle distribution of cells expressing GFP-C-TDP was not changed when compared with that of cells transfected with pEGFP empty vector, indicating that apoptosis is not induced in cells with formation of GFP-C-TDP aggregates. Taking these results together, it appears that overexpression of GFP-FL-TDP caused mild suppression of DNA synthesis and striking induction of apoptosis, whereas significant suppression of DNA synthesis and no abnormalities in the cell cycle were seen in cells including GFP-C-TDP aggregates. These results clearly indicate that cell death is induced via distinct molecular pathways upon overexpression of different TDP-43 species.

RNA pol II and some transcription factors are co-localized with TDP-43 inclusions and their activities are suppressed

It has been reported that transcriptional dysregulation is one of the central pathogenic mechanisms in Alzheimer's disease, Parkinson's disease and Huntington's disease (24). A number of transcriptional regulators, such as Sp1 and CREB, interact with protein aggregates, resulting in functional disruption of

these transcriptional factors in brain, followed by neurodegeneration (25–27). Therefore, to check whether these transcriptional factors are also associated with aggregates of TDP-43 CTF, we examined the localization of these factors as well as RNA pol II, which is a major enzyme responsible for transcription of protein-encoding genes. SH-SY5Y cells were transfected with GFP-C-TDP and incubated for 3 days, followed by immunohistochemical analyses. As shown in Figure 5A, inclusions composed of GFP-C-TDP were found to be positive for anti-RNA pol II antibody in cells expressing GFP-C-TDP. Furthermore, endogenous Sp1 and CREB were also co-localized with these inclusions. This result clearly shows that not only endogenous RNA pol II but also Sp1 and CREB are recruited to aggregated GFP-C-TDP. Next, we tried to confirm that endogenous RNA pol II interacts with TDP-43 biochemically. Cells expressing GFP, GFP-FL-TDP, GFP-N-TDP, GFP-C-TDP or GFP-ΔNLS-TDP were lysed in RIPA buffer and the lysates were subjected to immunoprecipitation with anti-GFP antibody-tagged Dynabeads, followed by immunoblotting using several antibodies. We found that endogenous RNA pol II bound with phosphorylated form of GFP-C-TDP to a greater extent than did GFP-FL-TDP, GFP-N-TDP and

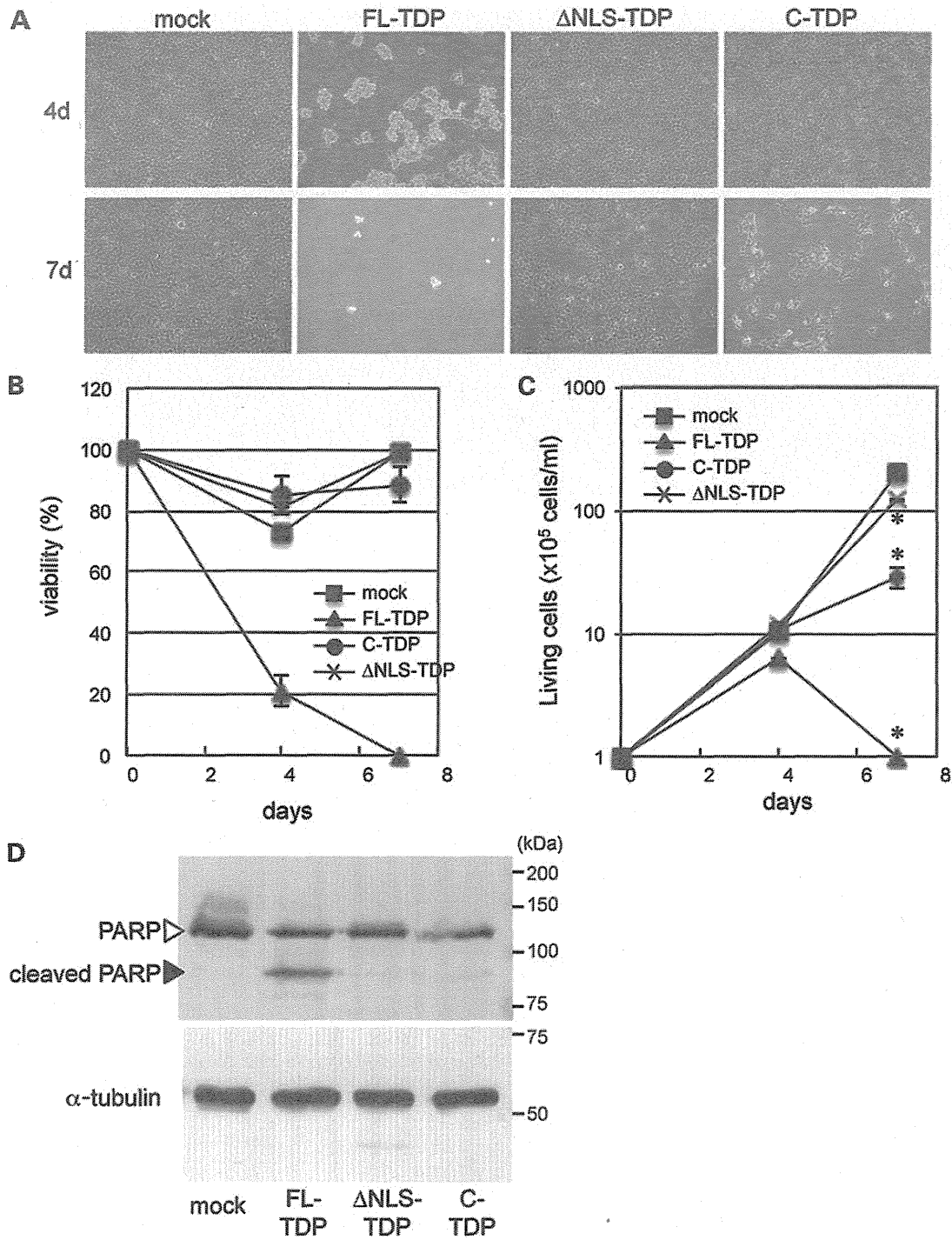


Figure 2. Cytotoxic effects of overexpressed TDP-43 in SH-SY5Y cells. SH-SY5Y cells were infected with each TDP-43 virus at 2×10^7 copies/well. At 4–7 days after infection, transfected cells were subjected to microscopic analyses, followed by cell death assay. They were assessed with light microscopy ($\times 10$ objective) at 4 and 7 days after transfection (A), and viability was examined by the trypan blue dye exclusion method (B) and living cells were counted using an automated cell counter TC10 (Bio-Rad) (C). The experiments were repeated three times; the illustrated results are typical. Data are means \pm SEM. * $P < 0.01$ versus ‘mock’ by Student’s *t*-test. (D) Transfected cells were also subjected to immunoblot analyses using anti-PARP and anti-tubulin antibodies. Note that PARP was cleaved in cells expressing FL-TDP, indicating that apoptosis is induced in these cells.

GFP-ΔNLS-TDP (Fig. 5B). We also examined the transcriptional activities of Sp1 and CREB in cells containing inclusions of GFP-C-TDP by means of luciferase assay. SH-SY5Y cells

were transfected with mCherry (mC)-tagged full-length (mC-FL), ΔNLS (mC-ΔNLS) or CTF of TDP-43 (162–414 residues, mC-C), followed by co-transfection of pFR-Luc together

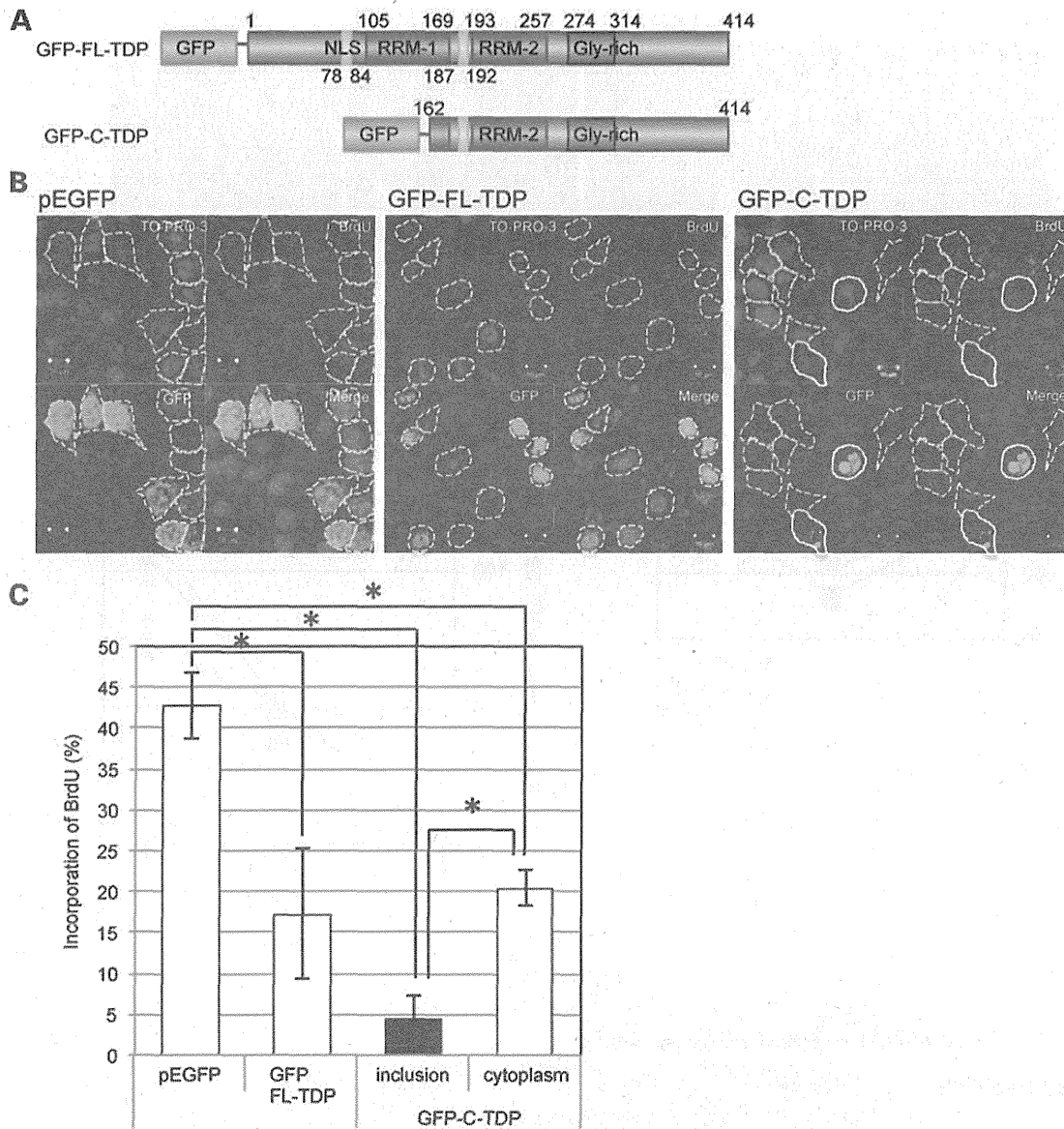


Figure 3. Comparison of cytotoxic effects of FL-TDP and its CTF. (A) Schematic representation of GFP-FL-TDP and GFP-C-TDP constructs in transient expression systems. (B and C) SH-SY5Y cells were transfected with the empty (pEGFP), GFP-FL-TDP or GFP-C-TDP vector for 3 days. After incubation, DNA synthesis was measured by BrdU uptake assay, using a confocal laser microscope (B). Scale bars, 10 μ m. The positions of cells are indicated with broken white lines. Cells with GFP-C-TDP inclusions are indicated with white lines. The ratio (%) of the numbers of BrdU-positive cells to the numbers of GFP-positive cells was calculated as the incorporation ratio of BrdU (C). At least eight areas per sample were analyzed ($n = 8-16$), and the experiments were repeated three times; the illustrated results are typical. Data are means \pm SEM. * $P < 0.01$ by Student's *t*-test.

with pGAL4-Sp1 or pGAL4-CREB. At 48 h after transfection, cells were harvested and the luciferase activity was measured. Figure 5C shows that the transcriptional activities of Sp1 and CREB were significantly suppressed not only in cells transfected with mC-C but also in cells expressing mC-FL. We also observed co-localization of GFP-FL-TDP with Sp1, as well as co-localization of GFP-FL-TDP with CREB (Supplementary Material, Fig. S2). However, transcriptional dysregulation caused by the expression of GFP-FL-TDP appears to be due to its high toxicity (Fig. 2B), rather than the co-localization. Alternatively, it is possible that cellular damage resulting from

overexpression of GFP-FL-TDP may cause transcriptional suppression of Sp1 and CREB.

RNA pol II co-localizes with TDP-43 inclusions in FTLD-TDP brain

To study the association of RNA pol II and transcriptional factors with TDP-43 aggregates in diseased brains, we carried out immunostaining of sporadic FTLD-TDP brain with several antibodies. As shown in Figure 6A and B, dystrophic neurites (DNs) were immunopositive for both anti-RNA pol II and

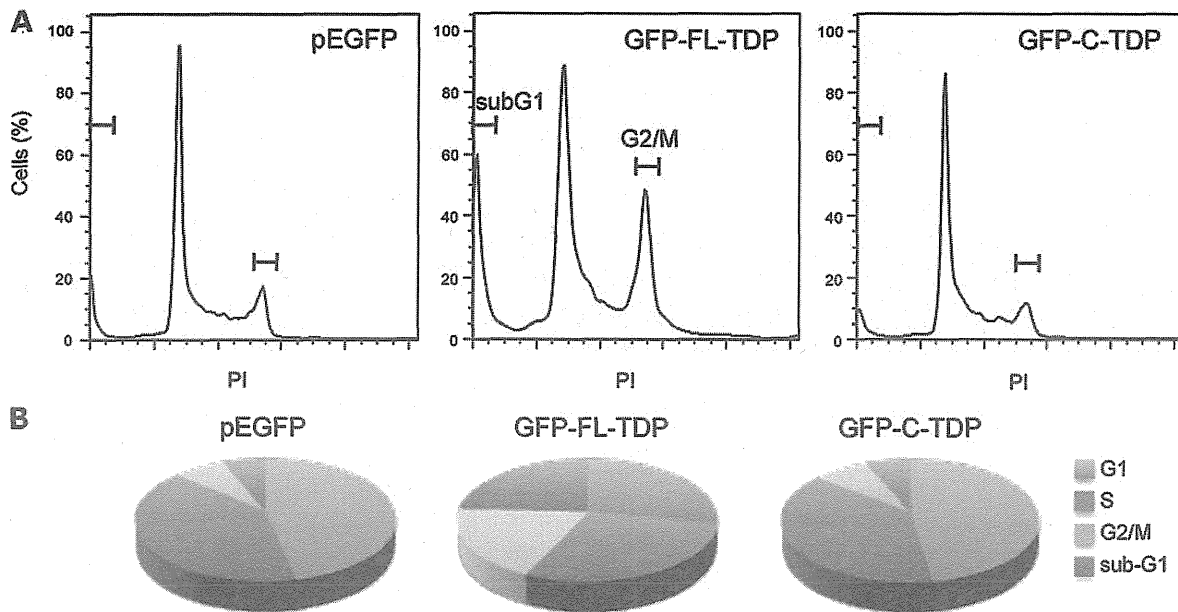


Figure 4. Analyses of the cell cycle distribution of cells transfected with GFP-tagged TDP-43. At 48 h after transfection of SH-SY5Y cells with GFP-tagged TDP-43 constructs or pEGFP empty vector, cells were stained with PI and analyzed with a flow cytometer. The results of flow-cytometric analyses are shown (A). The proportions of cells in G1, S, G2/M and subG1 phases were calculated using the Watson Pragmatic model (B). Note that growth arrest at G2/M phase was observed in GFP-FL-TDP-transfected cells, but not in GFP-C-TDP-transfected cells.

anti-pS409/410. In fluorescence-microscopic analyses, RNA pol II was co-localized with phosphorylated TDP-43 in DNs (Fig. 6D–F), clearly indicating that RNA pol II is indeed recruited to TDP-43 inclusions in FTLTDP brain as well as in cultured cells expressing GFP-C-TDP (Fig. 5A). On the other hand, unfortunately, antibodies to transcriptional factors Sp1, CREB and TAF II p130 failed to stain phosphorylated TDP-43 inclusions. These antibodies also failed to stain the nuclei of normal neurons in FTLTDP brains (data not shown). These results suggest the possibility that transcriptional activity is dysregulated *in vivo* as well as in cultured cells.

Apoptosis is not induced in FTLTDP brains

To test whether apoptosis is induced in FTLTDP brains, we performed immunoblot analyses of human brain lysates using anti-PARP and pS409/410 antibodies. As controls, we analyzed two control brains without any protein deposition and unaffected cerebellum of FTLTDP, in which no accumulation of TDP-43 and no atrophy has been reported. As shown in Figure 7, caspase-3-cleaved PARP was not detected in these control brains and the cerebellum of the FTLTDP case as well as in the temporal cortex of the FTLTDP case showing accumulation of TDP-43. This result indicates that apoptosis is not induced in affected neurons containing phosphorylated and aggregated TDP-43 *in vivo*.

DISCUSSION

Aberrant protein aggregates in affected neurons are well-known hallmarks of neurodegenerative diseases such as Alzheimer's disease and Parkinson's disease, but the mechanisms by which

these aggregates elicit neuronal degeneration remain unclear. In TDP-43 proteinopathy, inclusion bodies composed of phosphorylated, ubiquitinated and fragmented TDP-43 were found in neuronal cells of brains or spinal cords of patients. Recently, it was reported that prion-like propagation of aggregated TDP-43 is associated with the onset and progression of TDP-43 proteinopathy (22,28). So, in order to clarify the significance of TDP-43 inclusions in disease pathogenesis, we tried to establish cellular models with stable or transient TDP-43 expression in SH-SY5Y cells.

When we overexpressed FL-TDP in SH-SY5Y cells, significant cell death, suppression of cell growth, cleavage of PARP and increased cell populations at the G2/M and sub G1 phase were detected. However, intracellular inclusions of TDP-43 were not observed in these cells. These results suggest that an abnormally increased level of TDP-43, but not its aggregates, may be necessary for induction of cellular damage leading to apoptotic cell death. Indeed, several studies reporting that endogenous TDP-43 expression is tightly regulated and is critical for survival are consistent with this idea. For example, overexpression of wild-type TDP-43 caused motor neuron degeneration in yeast and rodents (15,17), knockout of TARDBP in mice led to embryonic lethality (29–32), heterozygous knockout mice develop motor impairments with age (30), and conditional knockout mice exhibit rapid postnatal lethality (29). TDP-43 is also regulated at the mRNA level through a negative feedback loop (3). These studies indicate that cellular TDP-43 levels are under tight control and perturbation of normal TDP-43 function is detrimental. Furthermore, it was reported that wild-type human TDP-43 expression causes mitochondrial aggregation in transgenic mice (33). This result suggests the possibility that apoptotic cell death found in cells expressing FL-TDP in this study may be caused by TDP-43-induced mitochondrial dysfunction.

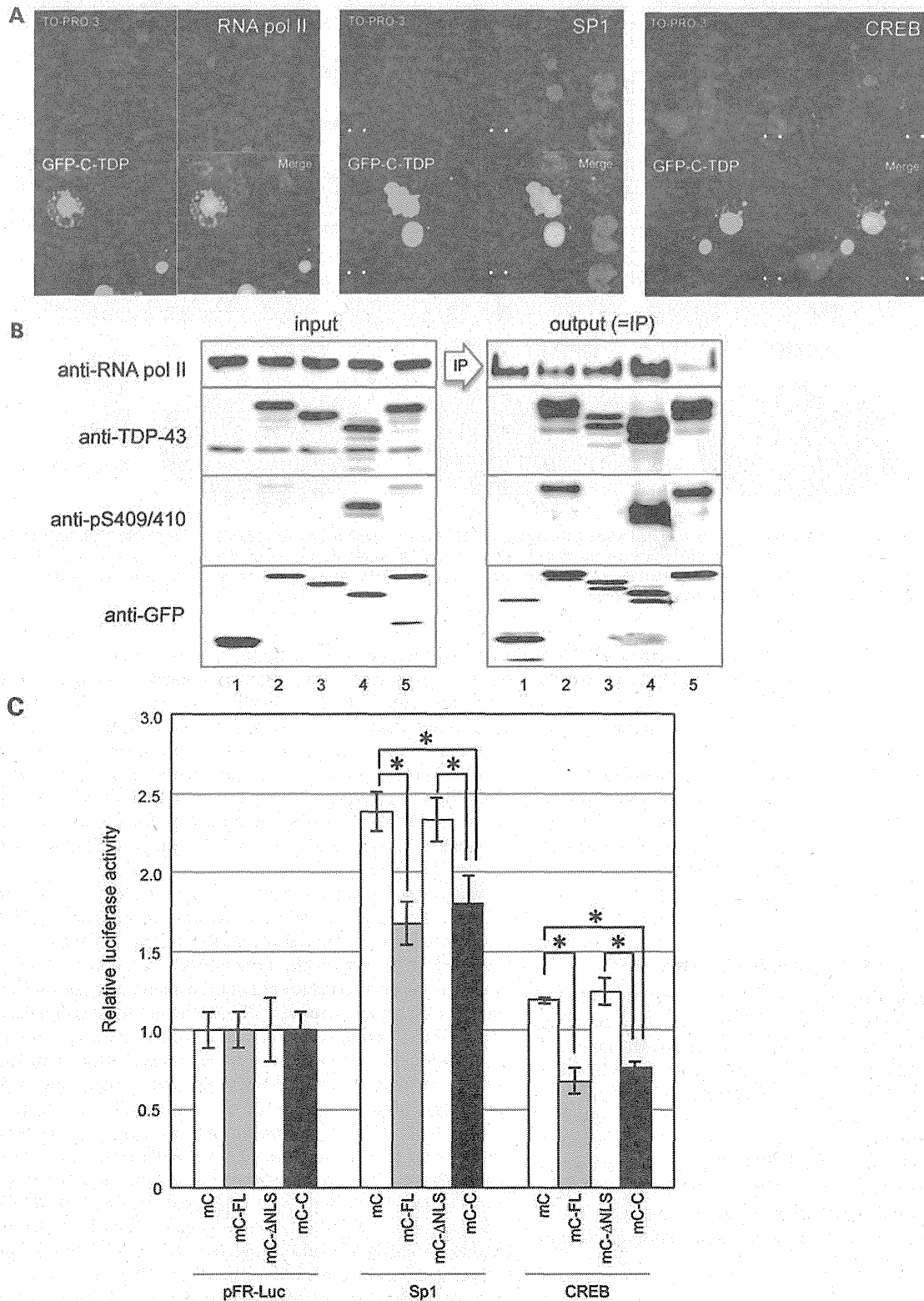


Figure 5. Co-localization of RNA pol II, Sp1 and CREB with intracellular inclusions of TDP-43 CTF. (A) At 72 h post-transfection with GFP-C-TDP, SH-SY5Y cells were stained with antibodies for RNA pol II, Sp1 and CREB, and observed with a confocal laser microscope. Scale bars, 5 μ m. (B) Immunoprecipitation of cells transfected with GFP-tagged TDP-43 was performed with anti-GFP, and each sample was subjected to immunoblotting with anti-RNA pol II, TDP-43, pS409/410 and GFP antibodies. 1: pEGFP; 2: GFP-FL-TDP; 3: GFP-N-TDP (TDP-43 N-terminal fragment of 1–161 residues); 4: GFP-C-TDP and 5: GFP- Δ NLS-TDP. (C) SH-SY5Y cells were transfected with mCherry (mC)-tagged Δ NLS-TDP-43 (mC- Δ NLS) or CTF (mC-C). On the next day, cells were co-transfected with pFR-Luc together with pGAL4-Sp1 or pGAL4-CREB. At 48 h after the second transfection, cells were collected and luciferase activity was measured. At least three points were measured for each sample ($n = 3-6$), and the experiment was repeated three times; the illustrated results are typical. Data are means \pm SEM. * $P < 0.01$ by Student's *t*-test.

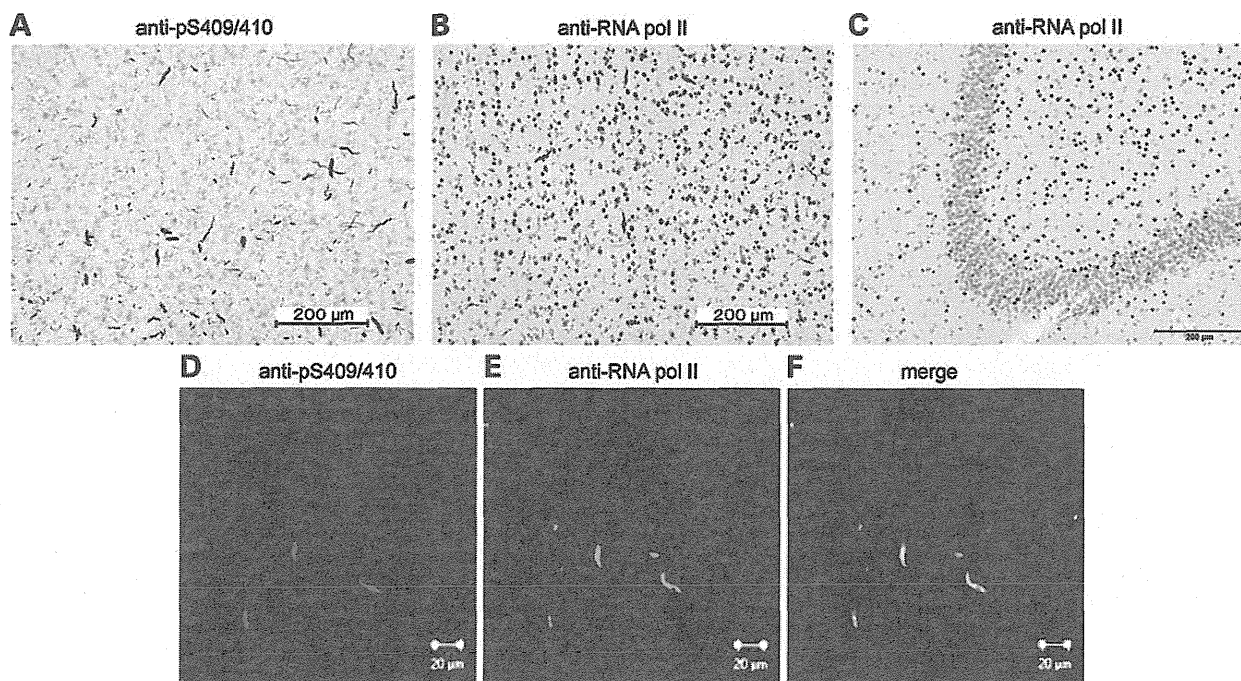


Figure 6. RNA pol II co-localizes with DNs in FTL D-TDP brain. Immunohistochemical stainings of sporadic FTL D-TDP (A and B) and control brain (C) were performed with anti-pS409/410 and anti-RNA pol II antibodies. (A–C) Bright-field images. Scale bars, 200 μ m. (D–F) fluorescence images of sporadic FTL D-TDP. (A and D), anti-pS409/410; (B, C and E), anti-RNA pol II; (F), merge of (D) and (E). Scale bars, 20 μ m.

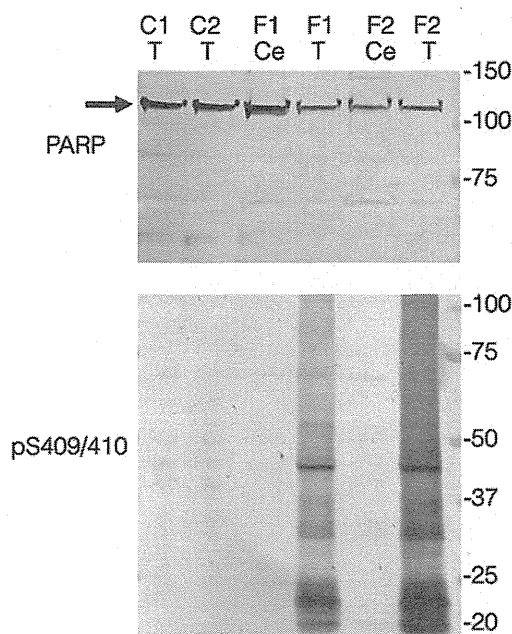


Figure 7. Apoptosis is not induced in affected neurons of FTL D-TDP brains. Immunoblot analyses of Tris-soluble (upper) and Sarkosyl-insoluble fraction (lower) prepared from human brain tissues (C1 and C2: control brains, F1 and F2: FTL D-TDP brains) were performed using anti-PARP (upper) and anti-pS409/410 (lower) antibodies. Ce, cerebellum; T, temporal cortex. Bands of endogenous whole PARP (\sim 120 kDa: arrow) were detected in controls and patients, but no caspase-cleaved band (\sim 95 kDa) was detected in affected or non-affected brains.

It remains unclear, however, how TDP-43 induces neuronal apoptotic cell death.

TDP-43 is a heterogeneous nuclear ribonucleoprotein and functions in RNA transcription and pre-mRNA splicing (34–38). In several genes, TDP-43 has been shown to bind directly to pre-mRNAs and regulate their splicing (36–42). In fact, widespread dysregulation of pre-mRNA splicing has been found in TDP-43-depleted cultured cells, TDP-43-depleted mouse brain and affected tissues from ALS patients (36–38, 41–44). These results suggest that dysregulation of pre-mRNA splicing is associated with ALS pathogenesis (38). Pre-mRNA splicing is mainly regulated by the spliceosome, which is a complex of small nuclear ribonucleoproteins (snRNPs) (38). The biogenesis of spliceosomes is regulated in Gemini of coiled bodies (GEMs) (38, 45–47). TDP-43 is likely to associate with GEMs in cultured cells (7), suggesting that TDP-43 contributes to GEM formation or function (38). Recently, it has been reported that the number of GEMs and the level of uridine-rich snRNA were decreased in spinal motor neurons of ALS patients (38, 48), suggesting that abnormal splicing caused by spliceosome disruption results in motor neuron death in ALS. Furthermore, several RNA processing genes have been shown to be mutated or genetically associated with ALS, including not only TDP-43, but also FUS/TLS, again suggesting that disordered RNA processing may be a key pathogenic mechanism in development of ALS (49). To our knowledge, the evidence presented here is the first to show that the formation of inclusions composed of TDP-43 CTF is cytotoxic: in cells with these inclusions, we observed a significant decrease of BrdU uptake, sequestration of RNA pol II, Sp1 and CREB into cytoplasmic aggregates of TDP-43 CTF, and

decreased transcriptional activities of Sp1 and CREB. Furthermore, RNA pol II was co-localized with these inclusions both in cultured cells and FTL-D-TDP brain. These results also support the idea that transcriptional deregulation plays a critical role in the degenerative cascade in TDP-43 proteinopathy.

Our results have shown that perturbation of the expression of FL-TDP elicits apoptotic cell death, and intracellular TDP-43 aggregation causes aberrations in RNA metabolism. The overproduction of TDP-43 might also lead to formation of intracellular TDP-43 aggregates, while decreased levels of TDP-43 protein could also influence TDP-43 expression, because TDP-43 itself auto-regulates its mRNA levels through a negative feedback loop (3). Intracellular TDP-43 aggregate formation may cause aberrant TDP-43 mRNA levels due to decreased levels of normal TDP-43 in nuclei, and this is known to be one of pathological characteristics found in brains of TDP-43 proteinopathy patients. On the other hand, lacking of apoptosis in FTL-D-TDP brains containing phosphorylated and accumulated TDP-43 observed in this study suggests that non-apoptotic cytotoxicity induced by TDP-43 aggregates rather than soluble TDP-43 may be closely related to the neurodegenerative mechanisms of TDP-43 proteinopathy. Therefore, it is likely that the loss of function and the gain of toxic function of TDP-43 are mutually associated with the onset of TDP-43 proteinopathy.

We conclude that dysregulation of FL-TDP expression causes neuronal apoptosis, while formation of intracellular aggregates of TDP-43 CTF induces defects in RNA metabolism. Our results suggest that plural pathways lead to TDP-43-induced cellular dysfunction, contributing to the degeneration cascades associated with onset of TDP-43 proteinopathy.

MATERIALS AND METHODS

Antibodies

A monoclonal antibody specific for TDP-43 (anti-TDP-43) was purchased from ProteinTech. An antibody specific for phosphorylated TDP-43 at both Ser409 and Ser410 antibodies (anti-pS409/410) were prepared as described (12,50). Anti-PARP antibody (#9542) was purchased from Cell Signaling. A monoclonal anti-RNA poly II antibody, which recognizes both the phosphorylated and non-phosphorylated forms of the C-terminal heptapeptide repeat region of RNA pol II, was purchased from Active Motif. A polyclonal anti-Sp1 antibody was purchased from Bethyl Laboratories and a monoclonal anti-CREB antibody (M01) was purchased from Abnova. Anti-GFP antibody was obtained from MBL (Nagoya, Japan). Anti-tubulin α antibody was purchased from Sigma-Aldrich. Anti-mouse IgM conjugated with Alexa-568 (A-21043) and anti-rabbit IgG conjugated with Alexa-568 (A-11011) were obtained from Molecular Probes.

Viral transduction of TDP-43 constructs

FL-TDP, NTF (1–161 residues: N-TDP) and CTF [162–414 residues: C-TDP (20)] of TDP-43 were subcloned into the pCL36-C1L-CMp-IRES-GFP lentivirus expression vector (51). HEK 293T cells were transfected with vector containing the insert or the empty vector along with Packing Mix (pCAG-kGP4.1R, pCAG4-RTR2 and pCAGGS-VSV-G vectors) for

40 h (with medium replacement after 6 h). Virus particles were pelleted by ultra-centrifugation (5800g, Beckman SE28 rotor, 16 h, 4°C). Viruses were then suspended in Hanks Balanced Salt Solution and stored at -80°C until use. For transfection, virus (1×10^7 copies/ml) was added to 2×10^5 SH-SY5Y cells/ml.

Cell culture and transfection

SH-SY5Y cells were cultured in DMEM/F12 medium (Sigma) supplemented with 10% fetal calf serum, penicillin–streptomycin–glutamine (Invitrogen), and MEM non-essential amino acid solution (Invitrogen). The cells were maintained at 37°C under a humidified atmosphere of 5% (v/v) CO_2 in air. They were grown to 50% confluence in six-well culture dishes for transient expression, and transfected with expression plasmids using FuGENE6 (Roche) according to the manufacturer's instructions. TDP-43 expression plasmids for FL-TDP and C-TDP were constructed as previously described (20,23).

Cell proliferation assay

Cell proliferation was determined with a 5-Bromo-2'-deoxyuridine Labeling and Detection Kit II (Roche). Transfected SH-SY5Y cells were grown on coverslips for 3 days, and then incubated for 10 h at 37°C in culture medium containing $10 \mu\text{M}$ BrdU. After incubation, cells were washed briefly, fixed and processed for immunostaining according to the manufacturer's instructions.

Cell cycle analysis

Cells were harvested at 72 h after transfection, fixed in 70% ethanol, treated with RNase A (1 mg/ml) for 30 min, and then stained with PI ($50 \mu\text{g/ml}$). DNA content was analyzed using an EPICS XL flow cytometer (Beckman Coulter).

Immunohistochemical analysis

SH-SY5Y cells were grown on coverslips and transfected as described above. After incubation for the indicated times, cells were fixed with 4% paraformaldehyde and stained with primary antibody (anti-TDP-43, anti-pS409/410, anti-RNA pol II, anti-Sp1 and/or anti-CREB antibody) at 1:1000 dilution. The cells were washed and further incubated with anti-rabbit IgG-conjugated Alexa-568 (1:1000), and then with TO-PRO-3 (1:3000, Invitrogen) or Hoechst 33342 (1:2000, Lonza) to counterstain nuclear DNA. Finally, they were analyzed using a LSM5 Pascal confocal laser microscope (Carl Zeiss).

Human brain tissues were obtained from Tokyo Metropolitan Institute of Medical Science (Tokyo, Japan). This study was approved by the local research ethics committee of Tokyo Metropolitan Institute of Medical Science (approval no. 12-3). Small blocks of human brain were dissected at autopsy or from fresh-frozen brain samples and fixed in 4% paraformaldehyde in 0.1 M phosphate buffer (pH 7.4) for 2 days. Following cryoprotection with 15% sucrose in 0.01 M phosphate-buffered saline (pH 7.4), blocks were cut on a freezing microtome at $30 \mu\text{m}$ thickness. The free-floating sections were incubated with anti-pS409/410 or anti-RNA pol II antibody for 72 h.

Following treatment with the appropriate secondary antibody, labeling was detected using the avidin-biotinylated horseradish peroxidase (HRP) complex system coupled with diaminobenzidine (DAB) reaction to yield a brown precipitate. In some sections, the DAB reaction was intensified with nickel ammonium sulfate to yield a dark purple precipitate. Moreover, the sections were incubated with secondary antibodies, labeled with FITC for anti-pS409/410 or with Rhodamine for RNA pol II and then observed under a fluorescence microscopy.

Immunoprecipitation and western blotting

SH-SY5Y cells grown in a six-well plate were transfected with GFP-tagged TDP-43 expression vectors (20). After incubation for 3 days, cells were harvested and lysed in TX buffer [50 mM Tris-HCl (pH 7.5), 150 mM NaCl, 5 mM ethylenediaminetetraacetic acid, 5 mM ethylene glycol tetraacetic acid (EGTA), 1% TX and protease inhibitor cocktail (Roche)] by brief sonication on ice. The lysates were incubated with anti-GFP antibody-linked Dynabeads (Invitrogen) for 4 h at 4°C. The immunoprecipitated Dynabeads complexes were washed five times with TX buffer. Proteins were eluted by boiling in SDS sample buffer and then processed for western blot analysis. Each sample was separated by 12% (v/v) SDS-PAGE using Tris-glycine buffer system, and proteins were transferred onto polyvinylidene difluoride membrane (Millipore). The blots were incubated overnight with each primary antibody at room temperature, followed by incubation with HRP-conjugated secondary antibody. Signals were detected using the ECL plus Western Blotting Detection System (GE Healthcare).

Luciferase assay

In the GAL4-Sp1 expression vectors, the 147 N-terminal codons of the yeast transcription factor GAL4 containing its DNA-binding domain were fused to fragments coding for the N-terminal regions of Sp1 and CREB. The expression vectors of pGAL4-Sp1 and pGAL4-CREB, and luciferase reporter plasmid pFR-Luc were prepared as described previously (52). SH-SY5Y cells were transfected with mCherry-tagged TDP-43 constructs. Next day, these cells were co-transfected with pFR-Luc together with pGAL4-Sp1 or pGAL4-CREB. At 48 h after the second transfection, cells were collected and luciferase activity was measured with a Luciferase Assay kit (Stratagene) according to the manufacturer's instructions. At least three points of each sample were measured ($n = 3-6$), and the experiment was repeated three times; the illustrated results are typical.

Preparation of human brain homogenates

Brain samples for immunoblot analyses were prepared as previously described (12,22). Briefly, frozen brain tissue from two controls or two patients with FTLTDP (type C) was homogenized in 10 volumes (w/v) of homogenization buffer (HB: 10 mM Tris-HCl, pH 7.4, 0.8 M NaCl, 1 mM EGTA and 10% sucrose). Aliquots of the homogenates were ultracentrifuged at 100 000g for 20 min at 4°C, and the supernatant was recovered as Tris-soluble fraction for immunoblotting analyses. Remaining lysate homogenates were incubated at 37°C for 30 min in HB buffer containing 2% Sarkosyl, and centrifuged at 20 000g for

10 min. The supernatants were ultracentrifuged at 100 000g for 20 min and the resulting pellets were used as Sarkosyl-insoluble fraction for immunoblotting analyses.

Statistical analysis

All values in the figures are shown as mean \pm SEM. Statistical analysis was performed using the unpaired, two-tailed Student's *t*-test. A *P* value of 0.01 or less was considered to be statistically significant.

SUPPLEMENTARY MATERIAL

Supplementary Material is available at *HMG* online.

ACKNOWLEDGEMENTS

We thank Drs Masami Masuda-Suzukake and Shin-ei Matsumoto for helpful comments and Dr Yoshinori Katakura for providing us pGAL4-Sp1, pGAL4-CREB and pFR-Luc plasmids.

Conflict of Interest statement. None declared.

FUNDING

This work was supported by a Grant-in-Aid for Young Scientists (B) (to M.Y., JSPS KAKENHI 24700370), a Grant-in-Aid for Scientific Research (S) (to M.H., JSPS KAKENHI 23228004), a Grant-in-Aid for Scientific Research on Innovative Area 'Brain Environment' (to T.N., MEXT KAKENHI 24111556) and a grant from Takeda Science Foundation (to T.N.).

REFERENCES

1. Arai, T., Hasegawa, M., Akiyama, H., Ikeda, K., Nonaka, T., Mori, H., Mann, D., Tsuchiya, K., Yoshida, M., Hashizume, Y. *et al.* (2006) TDP-43 is a component of ubiquitin-positive tau-negative inclusions in frontotemporal lobar degeneration and amyotrophic lateral sclerosis. *Biochem. Biophys. Res. Commun.*, **351**, 602–611.
2. Neumann, M., Sampathu, D.M., Kwong, L.K., Truax, A.C., Micsenyi, M.C., Chou, T.T., Bruce, J., Schuck, T., Grossman, M., Clark, C.M. *et al.* (2006) Ubiquitinated TDP-43 in frontotemporal lobar degeneration and amyotrophic lateral sclerosis. *Science*, **314**, 130–133.
3. Ayala, Y.M., De Conti, L., Avendano-Vazquez, S.E., Dhir, A., Romano, M., D'Ambrogio, A., Tollervy, J., Ule, J., Baralle, M., Buratti, E. *et al.* (2011) TDP-43 regulates its mRNA levels through a negative feedback loop. *EMBO J.*, **30**, 277–288.
4. Ayala, Y.M., Zago, P., D'Ambrogio, A., Xu, Y.F., Petrucelli, L., Buratti, E. and Baralle, F.E. (2008) Structural determinants of the cellular localization and shuttling of TDP-43. *J. Cell Sci.*, **121**, 3778–3785.
5. Buratti, E. and Baralle, F.E. (2008) Multiple roles of TDP-43 in gene expression, splicing regulation, and human disease. *Front. Biosci.*, **13**, 867–878.
6. Ou, S.H., Wu, F., Harrich, D., Garcia-Martinez, L.F. and Gaynor, R.B. (1995) Cloning and characterization of a novel cellular protein, TDP-43, that binds to human immunodeficiency virus type 1 TAR DNA sequence motifs. *J. Virol.*, **69**, 3584–3596.
7. Wang, I.F., Reddy, N.M. and Shen, C.K. (2002) Higher order arrangement of the eukaryotic nuclear bodies. *Proc. Natl. Acad. Sci. USA*, **99**, 13583–13588.
8. Ayala, Y.M., Pantano, S., D'Ambrogio, A., Buratti, E., Brindisi, A., Marchetti, C., Romano, M. and Baralle, F.E. (2005) Human, *Drosophila*, and *C. elegans* TDP43: nucleic acid binding properties and splicing regulatory function. *J. Mol. Biol.*, **348**, 575–588.